Supplementary Information (SI) for Physical Chemistry Chemical Physics.
This journal is © the Owner Societies 2026

Eu^{3+}-induced passivation and charge-transport modulation in $Cs_2FeCl_5·H_2O$ single crystals and evaporated thin films for photodetectors

Chen Wang,[a] Yu Li,[a] Huimeng Shen,[a] ,Jiayi Ren,[a] Qi Sun,[a] Hui Yan,[b] Li Xinpei,[c] Huawei Zhou,[*a] Xianxi Zhang,[*a] Federico Rosei,[*d] and Jun Zhang*[e,f]

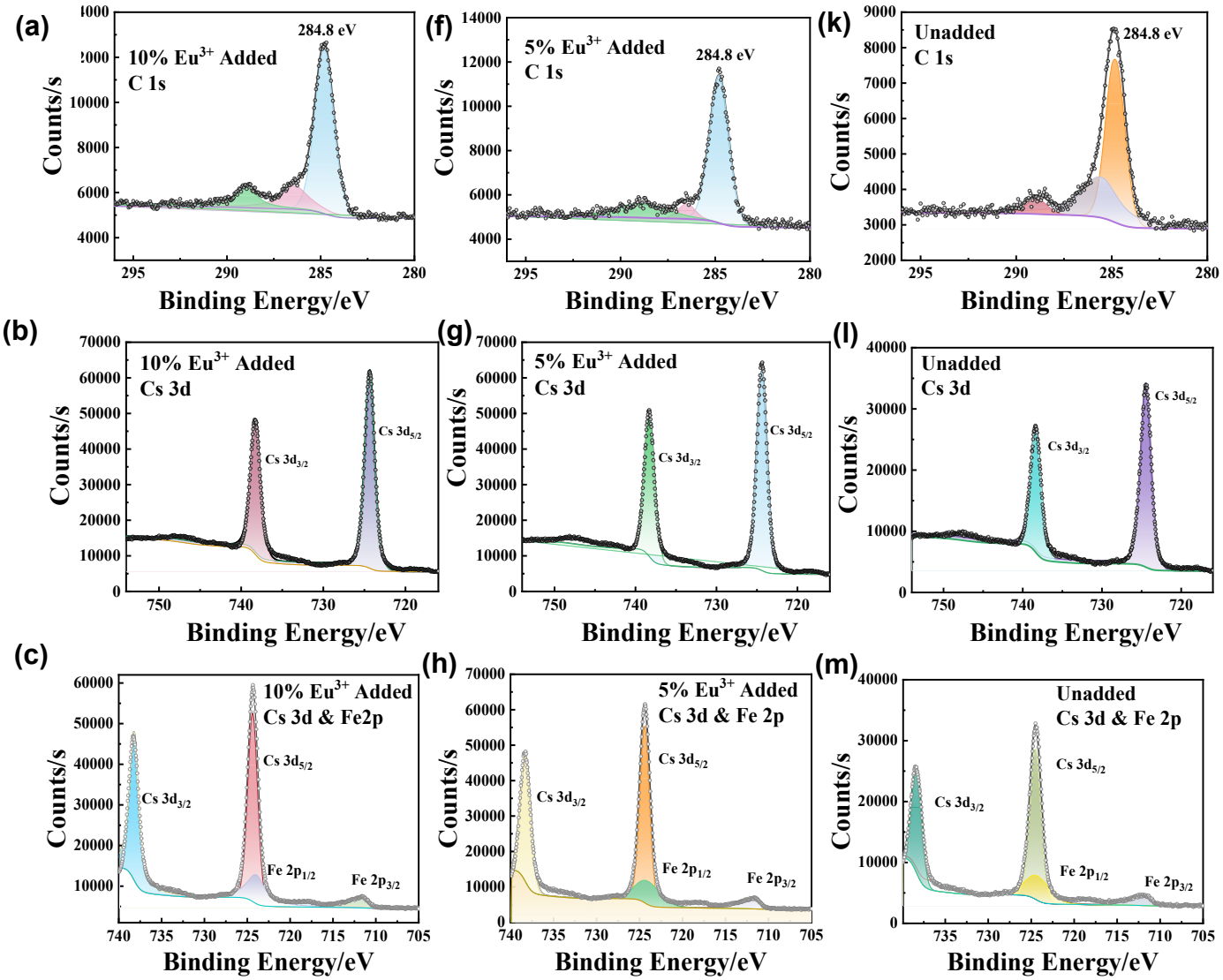

a.School of Chemistry and Chemical Engineering, Liaocheng University, zhouhuaweiopv@163.com; xxzhang3@126.com

b.State Key Laboratory of Macromolecular Drugs and Large-Scale Preparation, School of Pharmaceutical, Sciences and Food Engineering, yanhui@lcu.edu.cn

c.Shandong Jianzhu University 250011, China

d.Department of Chemical and Pharmaceutical Sciences, University of Trieste, Trieste 34127, Italy. E-mail: federico.rosei@units.it

e.National Rare Earth Functional Materials Innovation Center, Beijing 101400, China.

f.REF Rare Valley New Material Laboratory, Dalian 116001, China.

*Corresponding authors. E-mail addresses: zhouhuaweiopv@163.com; xxzhang3@126.com, federico.rosei@units.it

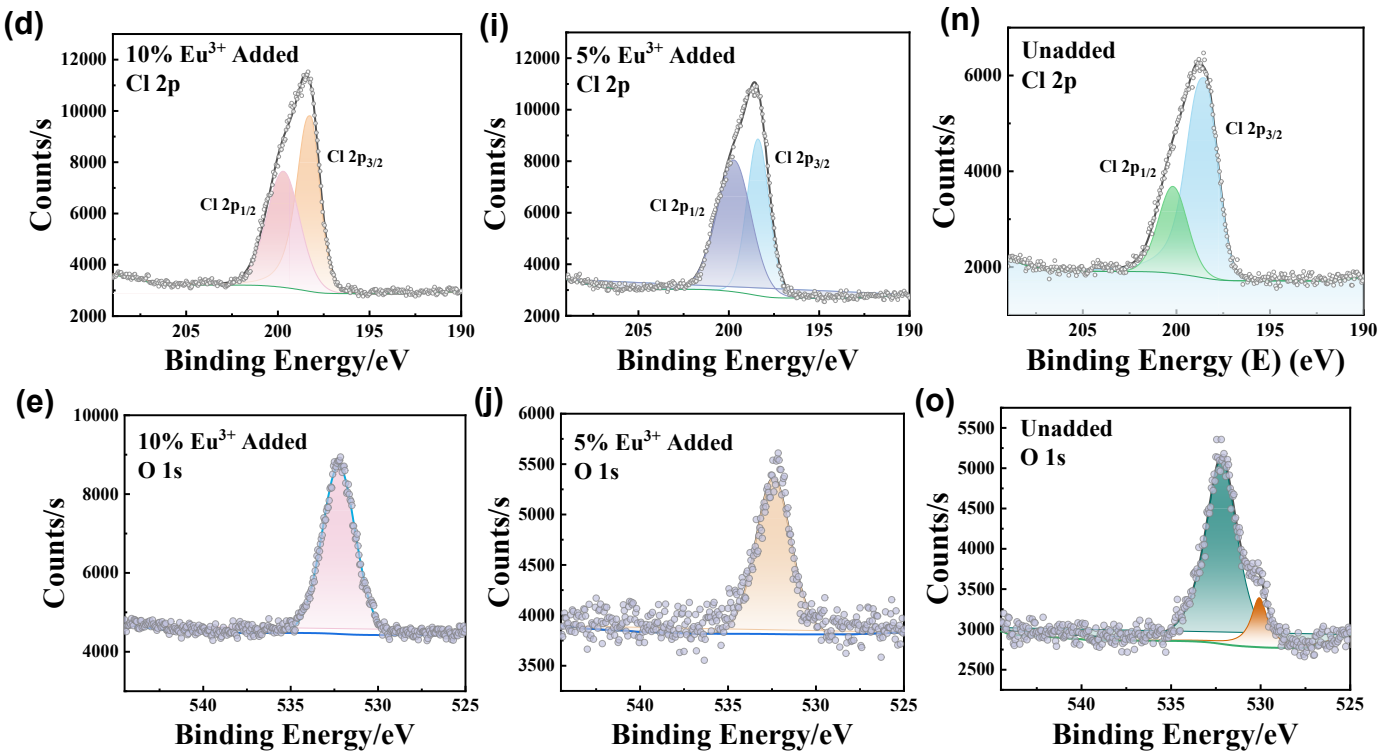

Figure S1. X-ray photoelectron spectroscopy (XPS) full survey spectrum of the sample, confirming the presence of Cs, Fe, Cl, C, O, and the Eu dopant elements. (a-e) 10% Eu added, (f-j) 5% Eu added, (k-o) unadded

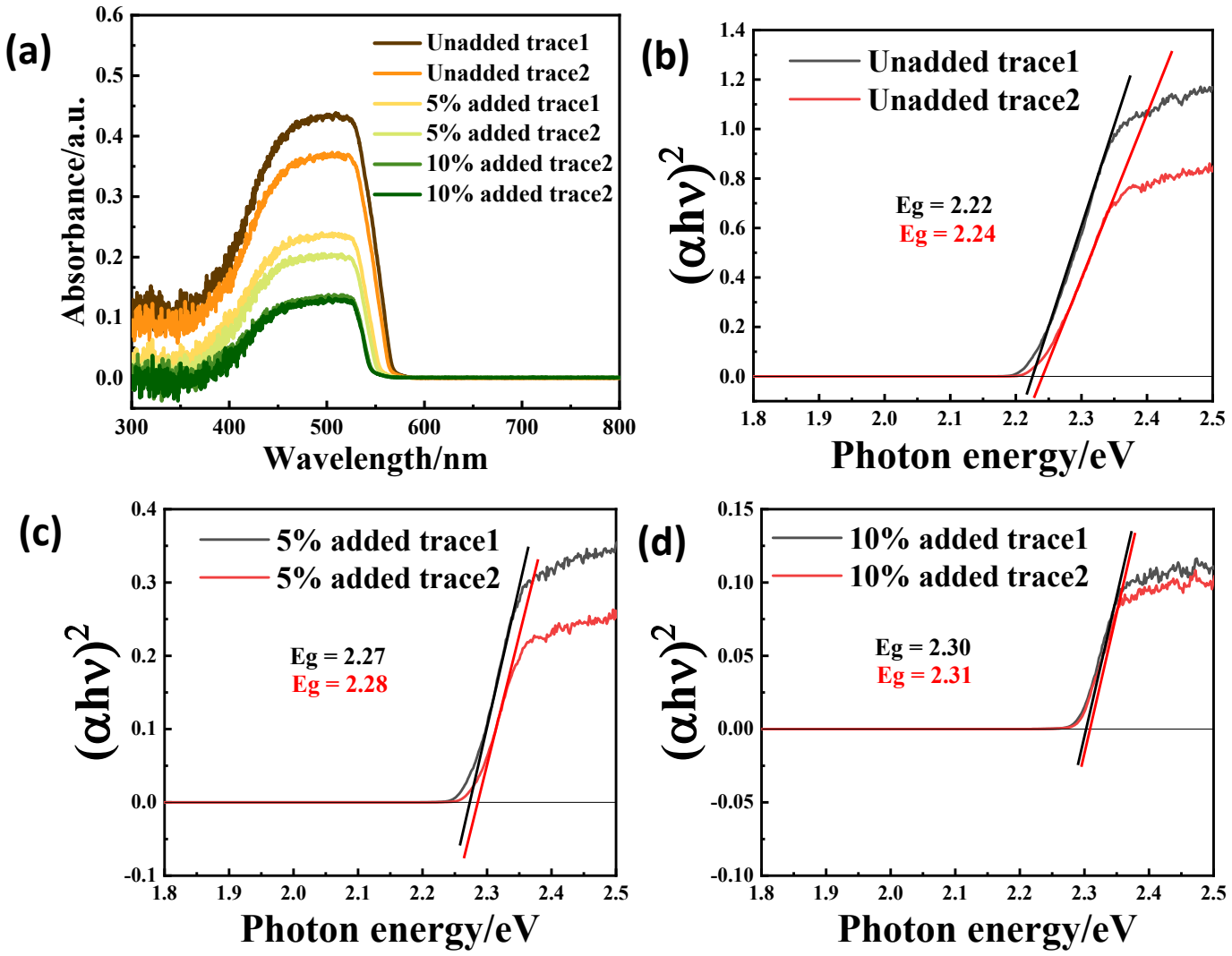

Figure S2. Reproducibility of the UV–Vis absorption and optical band-gap determination for unadded, 5% and 10%-added single crystals. (a) Absorption spectra of two independently grown crystals for each composition. (b–d) Corresponding Tauc plots of $(\alpha h\nu)^2$ versus photon energy and linear extrapolation used to extract the direct bandgaps.

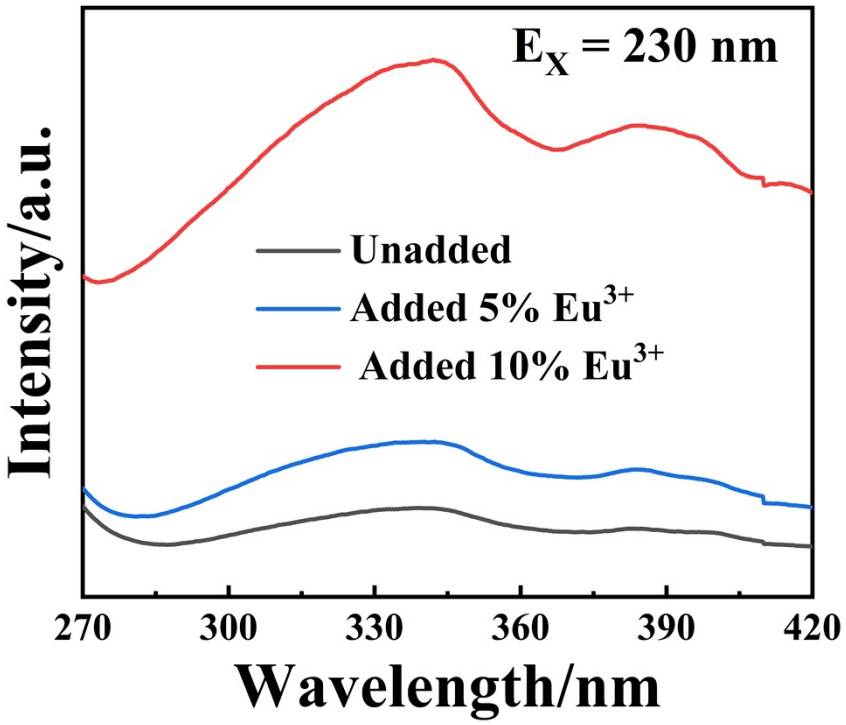

Figure S3. Reproducibility of spectra of unadded, 5% and 10%-added single crystals recorded under 230 nm excitation. All samples exhibit a broad emission band centred around 350 nm, while the overall PL intensity increases.

=

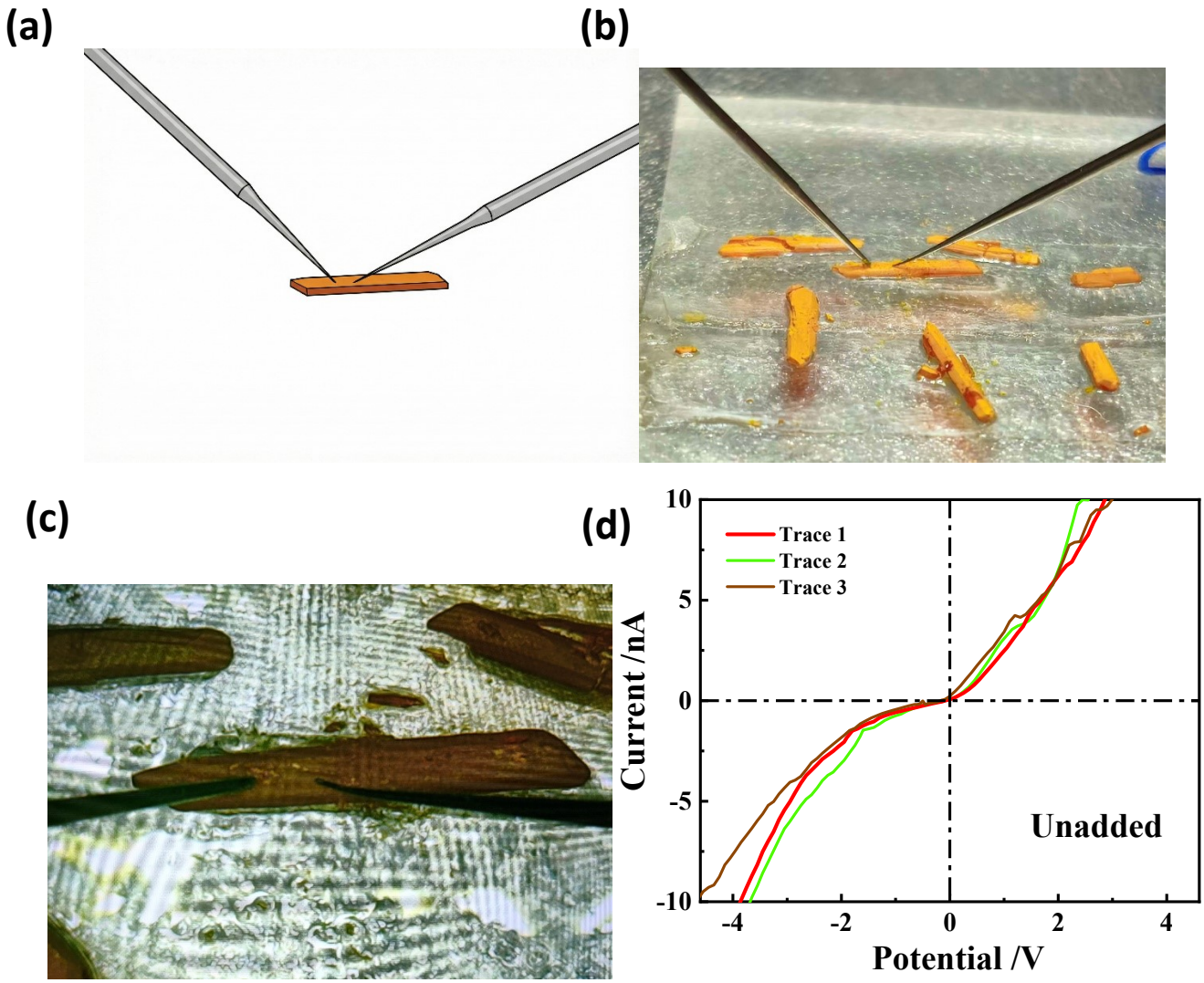

Figure S4. (a) Schematic illustration of the two-probe configuration used for single-crystal electrical measurements. (b,c) Optical image of the probe arrangement showing the macroscopic contact geometry. (d) Repeated I–V curves (Curve 1– 3) of an un-doped $Cs_2FeCl_5 \cdot H_2O$ single crystal.

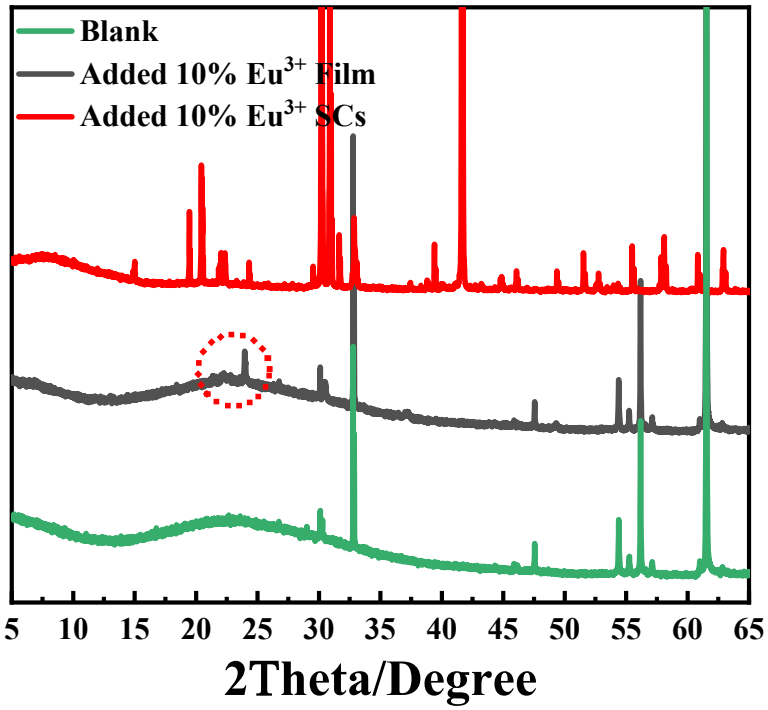

Figure S5. X-ray diffraction (XRD) pattern of the 10% Eu-added thin film prepared by the evaporation method

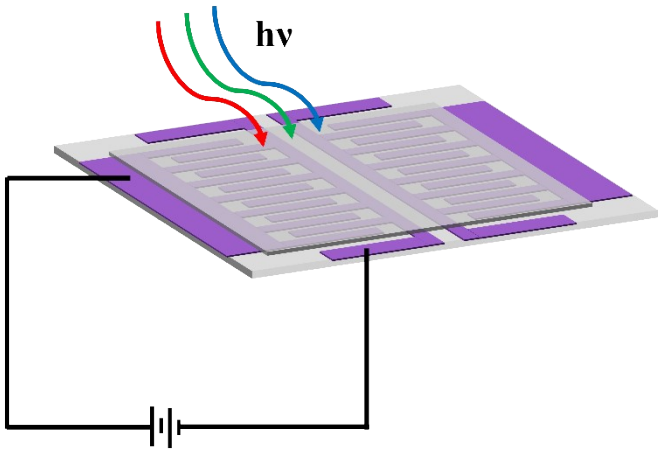

Figure S6. Schematic illustration of the photodetector structure based on ITO interdigitated electrodes.

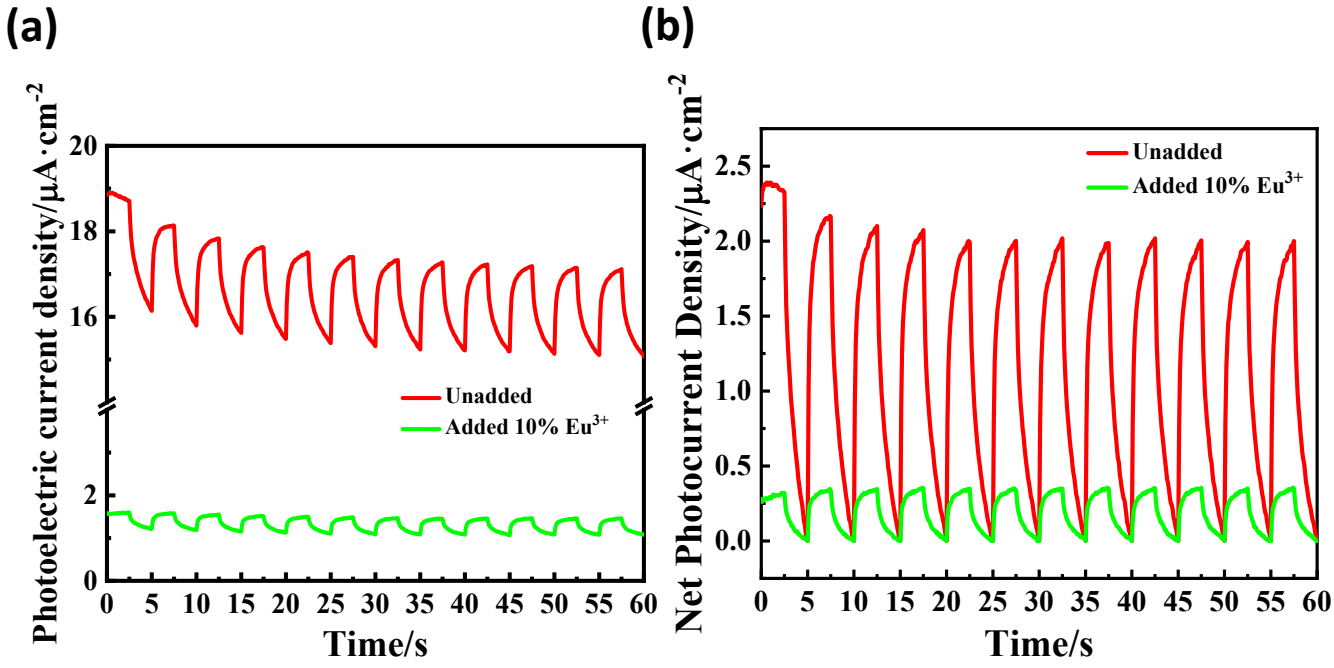

Figure S7. Final quantitative performance comparison of the undoped and 10% Eu^{3+} added devices under the optimal testing conditions (405 nm wavelength, 150 W/m^2 light intensity, and 5 V bias voltage.), (a) Photoresponse Curve and (b) Net Photocurrent Density Curve.

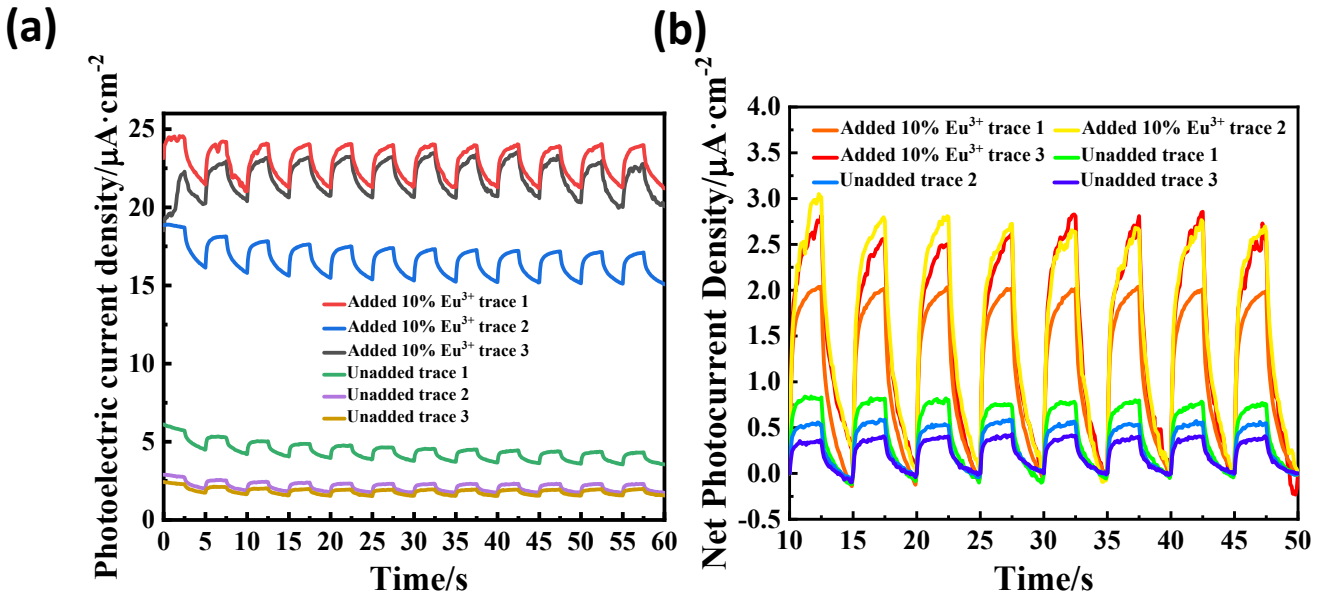

Figure S8. Final quantitative performance comparison of the undoped and 10% Eu^{3+}-doped devices under the optimised testing conditions (405 nm wavelength, 150 W m^{-2} light intensity and 5 V bias voltage). (a) Time-dependent photocurrent density showing three repeated traces for each device. (b) Net photocurrent density ($J_{light} - J_{dark}$) for the same set of measurements, highlighting the reproducibility of the photoresponse.

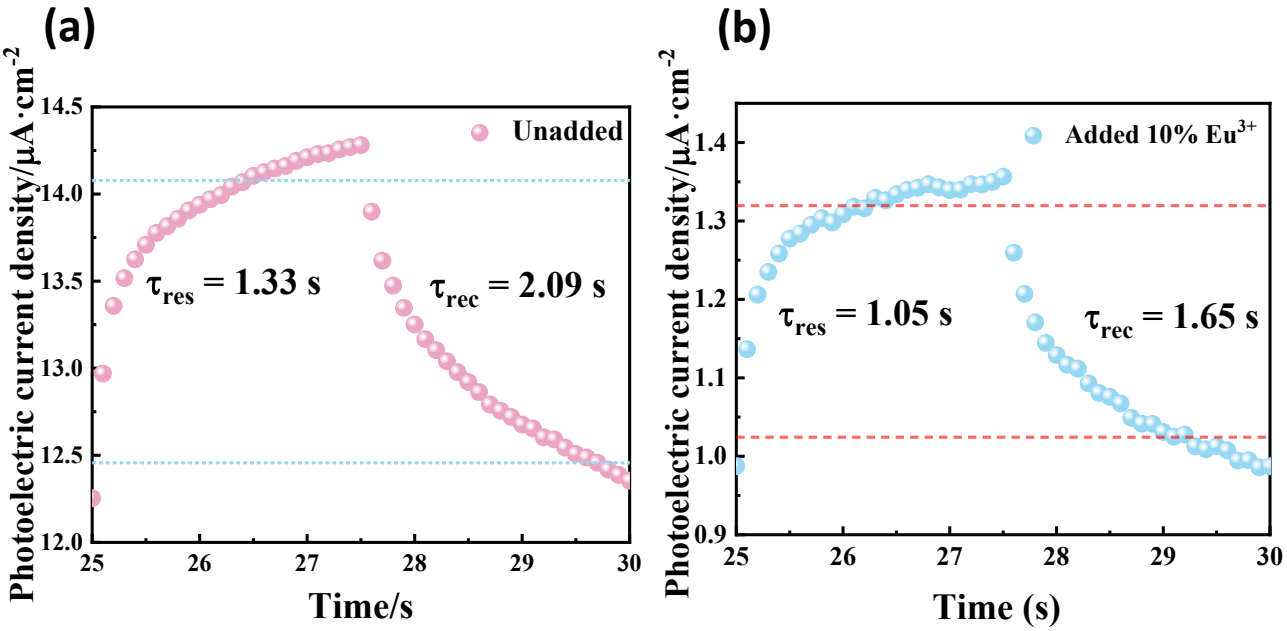

Figure S9. Photoresponse time analysis curves of the (a) undoped and (b) Eu^{3+}-added samples under 405 nm illumination, quantifying the photocurrent rise time (T_{res}) and decay time (T_{rec}).

Table S1. Crystallographic data and structure refinement details for pristine $Cs_2FeCl_5 \cdot H_2O$ and Eu-added $Cs_2Fe_{1-x}EuxCl_5 \cdot H_2O$ single crystals.

Empirical formula	**$Cs_2Fe_{1-x}Eu_xCl_5 \bullet H_2O$**	**$Cs_2FeCl_5 \bullet H_2O$**
Formula weight	521.74	516.94
Temperature	293(2) K	293(2) K
Wavelength	0.71073 Å	0.71073 Å
Crystal system, space group	Orthorhombic, Cmcm	Orthorhombic, Cmcm
Unit cell dimensions	a = 7.5011 (6) Å alpha= 90°.	a = 7.3059 (8) Å alpha= 90°.
	b = 17.3958 (18) Å beta= 90°	b = 17.2439 (17) Å beta= 90°
	c = 8.1013(8) Å gamma =90°.	c = 8.0207 (9) Å gamma =90°.
Volume	1057.12(17) $Å^3$	1024.30(19) $Å^3$
Z, Calculated density	4, 3.308 Mg/m^3	4, 3.352 Mg/m^3
Absorption coefficient	9.863 mm^{-1}	9.713 mm^{-1}
F(000)	939	924
Crystal size	0.4 x 0.25 x 0.18 mm	0.17 x 0.13 x 0.07 mm
Theta range for data collection	2.342 to 25.016 deg.	2.36 to 25.01 deg.
Limiting indices	0<=h<=8, 0<=k<=20, 0<=l<=9	-7<=h<=8,-20<=k<=20, -8<=l<=9
Completeness to theta = 25.016	100 %	99.8 %
Absorption correction	Semi-empirical from equivalents	Semi-empirical from equivalents
Max. and min. transmission	0.2701 and 0.1103	0.5496 and 0.2890
Refinement method	Full-matrix least-squares on F^2	Full-matrix least-squares on F^2
Data / restraints / parameters	547 / 60 / 31	526 / 1 / 33
Goodness-of-fit on F^2	1.381	1.205
Final R indices [I>2sigma(I)]	R1 = 0.072, wR2 = 0.2043	R1 = 0.0572, wR2 = 0.1291
R indices (all data)	R1 = 0.075, wR2 = 0.2068	R1 = 0.0608, wR2 = 0.1318
Largest diff. peak and hole	2.296 and -1.956 e • $Å^{-3}$	1.295 and -3.480 e • $Å^{-3}$